Nodeless pairing state in single-crystal YBa$_2$Cu$_3$O$_7$

Dale R. Harshman

Physikon Research Corporation, P.O. Box 1014, Lynden, Washington 98264 USA;*
Department of Physics, University of Notre Dame, Notre Dame, Indiana 46556, USA;
and Department of Physics, Arizona State University, Tempe, Arizona 85287-1504, USA

W. J. Kossler and X. Wan

Department of Physics, College of William and Mary, Williamsburg, Virginia 23187, USA

Anthony T. Fiory

Department of Physics, New Jersey Institute of Technology, Newark, New Jersey 07102, USA
and Bell Laboratories, Lucent Technologies, Murray Hill, New Jersey 07974, USA

A. J. Greer

Department of Physics, Gonzaga University, Spokane, Washington 99258, USA

D. R. Noakes and C. E. Stronach

Department of Physics, Virginia State University, Petersburg, Virginia 23806, USA

E. Koster

Department of Physics, University of British Columbia, Vancouver, British Columbia, Canada V6T 1Z1

John D. Dow

Department of Physics, Arizona State University, Tempe, Arizona 85287-1504, USA

Muon spin rotation (μ^+SR) measurements were conducted on a single crystal of YBa$_2$Cu$_3$O$_7$ with a superconducting transition temperature of $T_c \approx 91.3$ K and a transition width of $\Delta T_c < 0.5$ K in zero applied field. Data were taken at applied magnetic fields along the c axis of 0.05, 1.0, 3.0, and 6.0 T. We found, by taking into account the expected field-dependent and temperature-activated flux-line disorder, that our results were in fact consistent with a nodeless (s-wave) superconducting order parameter and that they appeared to be inconsistent with order parameters possessing nodes, such as those having $d_{x^2-y^2}$ symmetry. This result is consistent with early μSR measurements on sintered samples in which (we believe) strong pinning eliminated the temperature and field dependence of the vortex lattice disorder. These data (including their observed dependences on magnetic field) are, however, completely consistent with s-wave (or extended s-wave) pairing, provided that field-dependent and temperature-activated vortex depinning is also accounted for. Our results (i) confirm the s-wave superconductivity character originally observed in 1989, and (ii) show that the features of μSR (and microwave) data claimed by other authors to be evidence for d-wave superconductivity are instead symptomatic of temperature-dependent depinning of vortices, which results in long-ranged distortion of the flux lattice. Indeed, the probability that any published d-wave model gives a better fit than the two-fluid model is less than 4×10^{-6}.

I. INTRODUCTION

The pairing-state symmetry of the p-type high-T_c superconductors has been a subject of debate for several years: Are the hole carrier pairs s-wave or d-wave in character? Does the order parameter change sign with angle? Does the order parameter have nodes?

In 1991, Annett, Goldenfeld, and Renn[1] reviewed the experimental data for YBa$_2$Cu$_3$O$_{7-\delta}$ and concluded, with some caveats, that the pairing symmetry is likely conventional s-wave pairing. But in a 1996 review by two of the same authors, Annett, Goldenfeld, and Leggett,[2] a contrary opinion, that the pairing is likely d-wave, was put forth. Then in 2000, Annett and Wallington[3] offered yet another opinion that emphasized d-wave pairing. In this paper, we shall show

that the original determination of s-wave pairing in YBa$_2$Cu$_3$O$_{7-\delta}$ was correct,[4–7] and remains correct.[8,9]

In the original theory of Bardeen, Cooper, and Schrieffer (BCS),[10] the pairs are s-wave, and evidence for this was first provided for YBa$_2$Cu$_3$O$_7$ using muon spectroscopy over a decade ago, both in powders[4–6] and in crystals.[7] A comparable demonstration for Bi$_2$Sr$_2$CaCu$_2$O$_8$ was provided in 1991,[11] where s-wave-like behavior was recovered after the fluxon motion was reduced by high fields. More recently, a number of authors, most notably Van Harlingen,[12] Ginsberg,[13] Kirtley,[14,15] and Tsuei,[16–19] none employing muon spectroscopy, have argued that the pairing of holes in high-temperature superconductors is primarily of d-wave character. (See also Refs. 1, 2, and 3.)

Although *currently* most workers in the field seem to be-

69 174505-1

lieve that the pairing of holes in high-temperature superconductors has mostly *d*-wave character, only a few years ago the advocates of *s*-wave pairing were in the majority[4–8]—suggesting that any conclusion that the pairing is either *s*-wave or *d*-wave should be taken with caution. The situation is further complicated by the fact that what is *s*-wave in the bulk can be *d*-wave at the surface: Wave functions with significant character that is *s*-wave in the bulk, may become *d*-wave at the surface,[20] causing surface-sensitive experiments to reflect *surface d*-wave character for what is actually *bulk s*-wave behavior.

Moreover, the recent experiment executed by Li *et al.*[21,22] in response to a suggestion by Klemm[9] tested the *phase* of the wave function in $Bi_2Sr_2CaCu_2O_8$ and revived the *s*-wave viewpoint,[4–8] which, although championed by Dynes's group,[8] had been out of favor even for $Bi_2Sr_2CaCu_2O_8$, although not disproven. This experiment once more created uncertainty over whether the superconducting pairs are consistent with *s*-wave or *d*-wave superconductivity. There is, to date, no consensus on the matter, with the current leaders of the *s*-wave proponents being Harshman,[4,7] Pümpin,[5,6] Dynes,[8] and Klemm,[9] and the leaders of the *d*-wave superconductivity being Van Harlingen,[12] Ginsberg,[13] Kirtley,[14,15] and Tsuei.[16–19] No one claims that $YBa_2Cu_3O_7$ and $Bi_2Sr_2CaCu_2O_8$ have different angular momenta for the paired holes: To our knowledge, most researchers believe that in both bulk materials the paired holes have the *same* angular momenta; some authors favor *s*-wave pairing and others prefer *d*-wave.

Fortunately, there are perhaps *two basic ways* to determine the symmetry of the pairing in type-II superconductors: (i) from the magnetic penetration-depth $\lambda(T)$, measured by either muon spectroscopy,[23] microwaves,[24] or (rather imprecisely) by neutrons;[25] and (ii) from the phase of the wave function, as is done in a twisted bicrystal Josephson junction experiment. (See the discussion for *d*-waves by Refs. 12–19, and for *s*-waves by Ref. 9.) Both ways are subject to criticism: (i) The problem with the measurements of the magnetic penetration-depth $\lambda(T)$ is that it measures the length over which the magnetic fields inside the superconductor are attenuated, and as such, can be sensitive either to defects or to extrinsic effects, such as flux-motion, flux-pinning, or perturbations by magnetic ions; (ii) measurements of the phase of the wave function are subject to criticism if the measurement is surface sensitive (as is often the case) or if the sample contains some unexpected trapped magnetic flux, which can affect phase measurements. Since penetration-depth measurements performed using μ^+SR on $YBa_2Cu_3O_7$ have produced differing conclusions for the pairing: some *s*-wave,[4–6] others *d*-wave,[19,26–30] and others ambivalent about *s*- vs *d*-wave pairing,[31] we thought it would be best to reproduce the μ^+SR measurements of the basal-plane penetration depth $\lambda_{ab}(T,H)$ using *purer* $YBa_2Cu_3O_7$ samples, to determine if the data still favor the original *s*-wave interpretation of many years ago for $YBa_2Cu_3O_7$ (Refs. 4–7) and $Bi_2Sr_2CaCu_2O_8$.[11] After all, the muon measurements are *bulk sensitive*, whereas Josephson studies and other measurements of the wave-functions' phase (as well as photoemission and tunneling measurements) are rather sur-

face sensitive. In the rest of this paper, we focus on the bulk-sensitive muon studies.

The original penetration depth measurements of $YBa_2Cu_3O_7$ (Ref. 4) were performed with μ^+SR on sintered powders in 1987, and were clearly consistent with a nodeless gap (i.e., *s*-wave or extended *s*-wave pairing) and with a basal-plane magnetic penetration depth, $\lambda_{ab}(T\approx0)$ ≈ 140 nm. Several other investigations[5,6] subsequently confirmed the conclusions of Ref. 4. No comparisons were made at that time to show that those measurements were inconsistent with *d*-wave pairing (which was not yet in favor at the time).

Measurements of $\lambda_{ab}(T)$ on single crystals of $YBa_2Cu_3O_{7-\delta}$ (Ref. 32) were first reported in 1989,[7] and confirmed the earlier conclusion that the pairing state was either *s*-wave or extended *s*-wave for both the 90 K ($\delta \approx 0.05$) and the 60 K ($0.3 \leq \delta \leq 0.4$) bulk phases, but did not establish a bound on any *d*-wave contribution.[7,33] The main problem with the 1989 penetration depth measurements on the $YBa_2Cu_3O_7$ crystals was that the critical temperature was slightly low, 86 K (in zero applied field), which suggests that the measurements should be repeated on a better crystal with T_c above 90 K. It is important to point out, however, that in all of the earlier work, $\lambda_{ab}(T)$ tended to reflect the temperature dependence of the two-fluid model,[34] which indicated strong coupling, and *showed no linear-in-temperature dependence*, as expected for *d*-wave pairing.[29,30]

After the original work[4–7] on the pairing state of $YBa_2Cu_3O_7$, several other groups[26–28,35] began reconsidering data for $YBa_2Cu_3O_7$, based on the assumption that the absence of case-II coherence effects (such as the Hebel-Slichter anomaly[36–38]) necessarily implied higher angular momentum (other than *s*-wave) pairing. As we shall demonstrate, this assumption of higher angular momentum (e.g., *d*-wave) pairing is invalid.

Significant deviations from conventional *s*-wave behavior have been reported by other groups, based on μ^+SR data: Specifically, Sonier *et al.* have interpreted (incorrectly, as we shall show) their measurements of $\lambda_{ab}(T)$ performed well after 1991, on single crystals of $YBa_2Cu_3O_7$, as evidence for *d*-wave pairing.[35] Moreover, in their review article, Sonier, Brewer, and Kiefl[28] claimed that the earlier experiments on powders by Harshman *et al.*[4] and by Pümpin *et al.*[5,6] and on crystals[7] found consistency with *s*-wave pairing due to the misuse of Gaussian line shapes. This claim of Sonier *et al.* is contrary to the facts: (i) the single crystal data of Ref. 7 showed *s*-wave behavior and were fitted assuming a cutoff exponential, not a Gaussian, and (ii) it is a simple matter to show that the powder-averaged line shape generated by the internal magnetic field distribution of a vortex lattice is well approximated by a Gaussian, as has been well documented.[6] Since the qualitative *shape* of the magnetic-field distribution is independent of temperature, but the *width* varies with temperature, we expect the Gaussian fits of the data to produce linewidths that closely track the second moment of the field distribution as a function of temperature.

Moreover, the *s*-wave temperature dependence of the penetration depth λ_{ab} observed in the $YBa_2Cu_3O_7$ powder

experiments[4–6] and in the heavily twinned early single-crystal samples[7] likely reflected the true underlying pairing state: the extremely strong pinning forces clearly evident at and below T_c very likely suppressed any temperature-dependent reordering of the flux lines, as would occur if the pinning were weak (which is very likely the case in samples with $T_c > 90$ K).

As the quality of single-crystal samples has improved from 1989 to the present, flux pinning in the best crystals should have become *weaker*; this has introduced the possibility of temperature-dependent fluxon reordering in the best samples now available. Such fluxon reordering has already been observed in high-quality $Bi_2Sr_2CaCu_2O_8$ crystals, where strong temperature and field effects on μ^+SR data were found,[11] reflecting weak pinning. Very similar temperature and field dependences are observed in the present work for our higher-quality $YBa_2Cu_3O_7$ samples, which we shall show are indicative of flux pinning, not due to d-waves or $L \neq 0$ angular momenta.

In this work we first discuss (Sec. II) how the experiment was performed and analyzed. Then we prove (Sec. III A) that neither s-wave pairing nor d-wave pairing *alone* can explain the current data from muon spectroscopy. Then we consider pairing (either s-wave or d-wave) in combination with vortex pinning (Sec. III B). In Sec. III C we introduce our collective pinning model. And in Sec. III D we show that s-wave pairing plus flux pinning does describe the data rather well. And finally, Sec. III E is devoted to d-wave pairing plus flux pinning, which fails to fit the data. Section III F contains a discussion of data from other probes, data which cast doubt on the d-wave interpretation. Our conclusions are developed in Sec. IV.

Hence, we show that the deviations from s-wave pairing could be associated with temperature-dependent flux-pinning phenomena, not with d-wave pairing. To accomplish this, we first present μ^+SR data acquired on a high-quality $YBa_2Cu_3O_7$ crystal at applied magnetic fields of 0.05, 1.0, 3.0, and 6.0 T. The temperature and field dependences of the internal field distributions are carefully compared using a self-consistent analysis in which deviations from s-wave symmetry behavior are attributed to weak flux-pinning phenomena, rather than to d-wave effects. We argue that the purported intrinsic d-wave behavior previously claimed for muon experiments is probably not due to d-waves, but is an extrinsic phenomenon caused by flux pinning.

II. EXPERIMENT

The $YBa_2Cu_3O_{6.95}$ crystal measured for the present work was grown in a Y-stabilized ZrO_2 crucible according to methods described elsewhere.[39] The sample exhibits a transition temperature of $T_c \approx 91.3$ K, has a transition width of $\Delta T_c < 0.5$ K (in zero applied field), and has dimensions $5 \times 4 \times 0.75$ mm^3, dimensions which correspond to a demagnetization coefficient of about 0.793 for magnetic fields applied along the c axis.[40]

The μSR experiments were conducted on the M20 and M15 secondary channels of the TRIUMF cyclotron facility in Vancouver, British Columbia, Canada, using the LAMPF

(low-field) and Belle (high-field) spectrometers. The time-differential technique used in these studies is described elsewhere,[41] so only a brief description will be presented here.

Positive muons (4.2 MeV) are stopped in the sample, where they decay (muon lifetime $\tau_\mu \approx 2.197$ μs) with each emitting a positron preferentially along its final spin-polarization direction. A clock is started when the incident muon enters the sample, and is stopped upon the detection of the decay positron. Since the muons are created via pion decay at rest, with spins antiparallel to their momenta, the time evolution of the muon spins can be measured. Typically, one measures the time evolution of millions of positive muons' spins (one at a time), yielding an ensemble average. Standard magnetic-field geometries allow the application of fields in directions parallel (longitudinal) or perpendicular (transverse) to the initial muon polarization. In the present work, only transverse-field measurements are employed, yielding a relaxation function, $G_{xx}(t)$, consisting of a relaxation envelope modulating a precessing muon spin amplitude [see Eq. (5) below]. This is analogous to free-induction decay in nuclear magnetic resonance. To allow for measurements in high transverse fields, the muon spins are rotated $\sim 90°$ (by an $\mathbf{E} \times \mathbf{B}$ filter) and the field is applied parallel to the incident beam momentum vector (thus still conforming to a transverse-field geometry), which also helps focus the incident muon beam. Since only one muon is in the sample at a time, there are no complications due to μ^+-μ^+ interactions.

For the present experiments, data were taken at applied magnetic fields along the c direction of 0.05, 1.0, 3.0, and 6.0 T. About 10^7 total muon-decay events were accumulated at each temperature (the temperatures were held to an accuracy of better than 0.1 K) and at each field. The fields were accurate to better than 5×10^{-5} T.

For the analysis of the μSR data presented here, we first compared the data with the Ginzburg-Landau model of Ref. 42 and then with the more conventional London model,[43] with an added Gaussian cutoff, as defined in Eq. (1) below. While the fit qualities were indistinguishable between these two models, the coherence distance and the penetration depth parameters were found to be very strongly correlated with each other in the Ginzburg-Landau case. This correlation undoubtedly led to the factor of 3 or 4 variation in the coherence distance with magnetic field reported by Sonier *et al.*,[26,28] when one should have expected the vortex core size to vary only about 20% (Ref. 44) over the same field range. Moreover, the field dependence in the penetration depth and coherence distance that Sonier *et al.* found in fitting the theory of Ref. 42 to their data is contrary to the theoretical assumption that they are constants.

Since our primary goal is to accurately extract the second moment of the vortex lattice field distribution as a function of both temperature and field, we have chosen to adopt a spatial field distribution of the London form,[43]

$$B(\mathbf{r}) = B\Sigma_{\mathbf{g}} \exp(i\mathbf{g} \cdot \mathbf{r}) \; (1 + \lambda^2 g^2)^{-1} \exp(-\tfrac{1}{2}\xi_0^2 g^2), \quad (1)$$

where B is the average internal field, $\mathbf{g}$ is a reciprocal lattice vector for a triangular vortex lattice, λ is a parameter which

under ideal conditions would equal the magnetic penetration depth, and we have added a core cutoff at small **r** with a cutoff distance ξ_0. To avoid the problem of coherence-parameter and penetration-depth correlation (discussed above), and to circumvent anomalous results for the field dependence of the coherence distance,[26,28] the cutoff parameter ξ_0 was fixed at 0.1 nm for all four fields analyzed (i.e., all vortices were assumed to be virtually point vortices[45]).

In order to obtain the relaxation function $G_{xx}(t)$, we first found the field probability distribution function, $n(b)$, as numerically derived from Eq. (1) by determining the area of a vortex lattice unit cell that falls between magnetic fields b and $b+db$. Thus $n(b)$ was obtained from

$$n(b) = \int \delta(b-b')dA(b') \Big/ \int dA(b'), \qquad (2)$$

where $dA(b')$ is an elemental piece of the vortex lattice unit cell for which the field is b' and the unit cell has a total area of $\int dA(b')$.

Once $n(b)$ is known, the relaxation function arising from the vortex lattice (vl) is then given by the cosine transform,

$$G_{xx}^{vl}(t) = \int \tilde{n}(b;\sigma_M)\cos(\gamma_\mu bt+\phi)db, \qquad (3)$$

where b is the field sensed by the muon, ϕ is the initial phase, γ_μ ($=2\pi\times 13.55342$ MHz/kG) is the muon gyro-magnetic ratio, and $\tilde{n}(b;\sigma_M)$ is given by

$$\tilde{n}(b;\sigma_M) = N^{-1}\int n(b')\exp(-[b-b']^2/2\sigma_M^2)db'. \quad (4)$$

Here $\sigma_M(T,H)$ is the smearing parameter determined by fitting the data to Eq. (5) below, and N^{-1} is a normalization constant. The Gaussian convolution, Eq. (4), is employed to account for the variation in the local average field arising from vortex lattice distortions.

Finally, the complete asymmetry function $G_{xx}(t)$ used for fitting the data is constructed by adding to $G_{xx}^{vl}(t)$ a Gaussian decaying signal to describe the small signal from the muons which stop outside the superconducting sample, but are not vetoed by the electronics. Defining f to be the fraction of the total spectrum arising from muons stopped inside the superconducting sample, we have

$$G_{xx}(t) = fG_{xx}^{vl}(t) + (1-f)\exp(-\Delta^2t^2/2)\cos(2\pi\nu t+\phi). \tag{5}$$

Here Δ is the decay rate and ν is the precession frequency for muons stopped outside the sample, and ϕ is, again, the initial phase. The raw spectra for all of the fields measured were fit[46] assuming the function given in Eq. (5). In the case of the 6.0 T data, no background component was present (i.e., $f = 1$), but for 0.05, 1.0 and 3.0 T, f is 0.95, 0.84 and 0.96, respectively.

From this analysis, the fitting parameters, $\sigma_M(T,H)$ and $\lambda(T,H)$ were obtained. These parameters model the randomly broadened vortex lattice field distribution, and can be used to obtain experimental results for the deformation of the
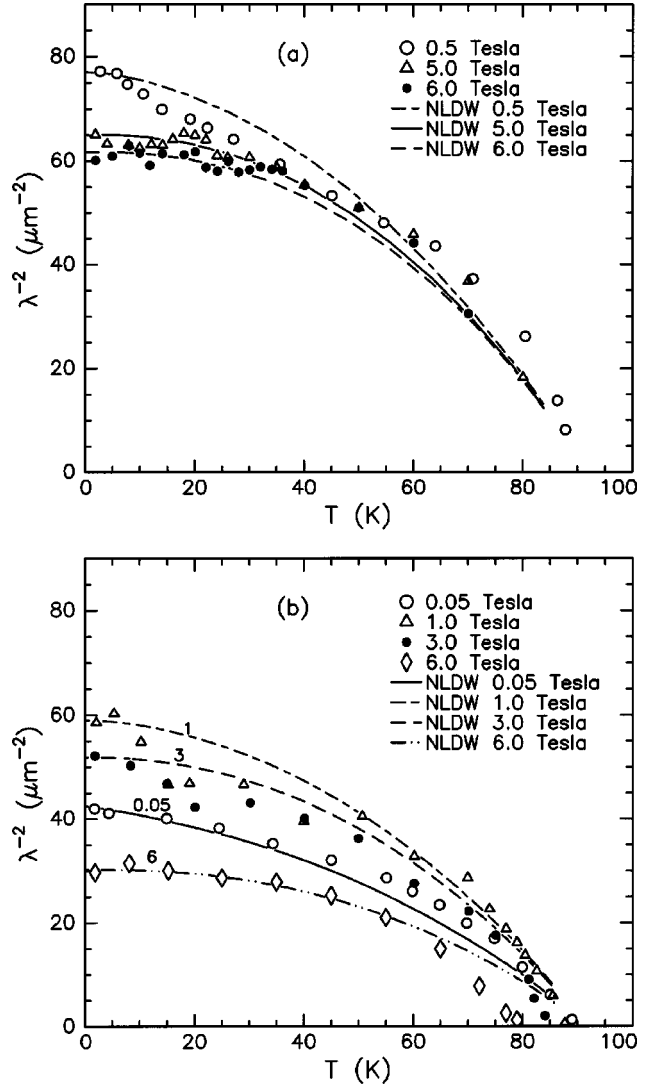

FIG. 1. Comparison of the d-wave theory for the effective magnetic penetration depth $\lambda(T,H)$ of Ref. 30 with (a) the fitted λ data of Fig. 3 from Ref. 30, and (b) the present data with fitted λ parameter. The curves in frame (a) are as given in Ref. 30 for $\kappa=65$ and $\lambda(T=0,H=0)=107.8$ nm. The parameter values necessary to compare with the data in part (b) are $\lambda(T=0,H=0)=151.5$, 120.0, 120.5, and 147.5 nm for $H=0.05$, 1.0, 3.0, and 6.0 T, respectively. As discussed in the text, a comparison could not be made with a universal value of $\lambda(0,0)$.

magnetic field distribution of the ideal (perfect) vortex lattice in the presence of perturbations (e.g., flux pinning), which we treat in Sec. III.

III. RESULTS AND INTERPRETATION

Figure 1 shows λ^{-2}, the inverse square of the penetration-depth parameter λ, as a function of temperature T for (a) the data provided in Ref. 30 for $H=0.5$, 4.0, and 6.0 T, and (b) our data for applied fields H of 0.05, 1.0, 3.0, and 6.0 T. Bear in mind that λ is a fitted parameter and is not necessarily the actual magnetic penetration depth, λ_{ab}. While these two sets of data, (a) and (b), have some similar features, there are significant quantitative differences, which suggest that some extrinsic effects play a significant role in

shaping them. Specifically, (i) the data in Fig. 1(a) are systematically greater than those in Fig. 1(b); (ii) there is a distinctive inflection point in λ^{-2} versus temperature near $T \approx 20$ K, which is most evident at intermediate fields [i.e., $H = 0.5$ T in Fig. 1(a) and $H = 1.0$ and 3.0 T in Fig. 1(b)]; and (iii) a nonmonotonic dependence of $\lambda^{-2}(T \rightarrow 0, H)$ on applied magnetic field H is shown in Fig. 1(b). The curves in Fig. 1(a) are the same as those given in Ref. 30 for $\kappa = 65$ and a value of $\lambda(T \approx 0, H = 0) = 107.8$ nm. However, a comparison of the same theory[30] with the data in Fig. 1(b) is not possible with a universal value of $\lambda(T \rightarrow 0, H = 0)$, due primarily to the nonmonotonic behavior in H of $\lambda^{-2}(T \rightarrow 0, H)$, and the fact that $\lambda^{-2}(T, H)$ at the lowest fields [i.e., 0.05 T in Fig. 1(b)] is not linear in temperature, as predicted in Ref. 30. The parameter values necessary to ''reasonably'' compare the d-wave model of Ref. 30 with the data in Fig. 1(b) are given in the figure caption.

A. Neither s-wave pairing nor d-wave pairing alone fits the data

It is clear that the data of Fig. 1 for λ^{-2} cannot be adequately explained with an s-wave model alone. It is equally clear, from the comparison with theory shown in Fig. 1, that the d-wave model alone does not (and cannot) describe the data particularly well either. Consequently, it was surprising to us that Sonier *et al.*, citing similar data, claimed that d-wave pairing accounts for the observed deviations of λ^{-2} from a ''conventional'' s-wave model's temperature dependence. Indeed Amin *et al.*,[30] upon comparison of their nonlocal d-wave theory with μ^+SR data provided by Sonier, found poor agreement and stated (referring to their theoretical prediction for λ^{-2}), ''The main discrepancy between the theory and experiment in Fig. 3 (of Ref. 30) is the lack of linearity (in temperature of the theory for λ^{-2}) at 0.5 T; however, it is difficult to envision how nonlinear corrections could cure this.'' In making this statement, Amin *et al.* acknowledged that the d-wave theory does *not* explain the μ^+SR data. In fact, while the nonlocal d-wave theory of Ref. 30 *does* predict $\lambda(T \rightarrow 0, H)$ to be linear in field H at 0.05 T, the data of Fig. 1(b) do not bear this out. It should also be noted that the value of $\lambda(0,0)$ (= 107.8 nm) necessary to compare with the μ^+SR data [Fig. 1(a)] (Ref. 30) is significantly smaller than the well established value.[47]

Interestingly, although the data of Sonier *et al.* for $H = 0.5$ T (Ref. 30) appear to be somewhat ''linear'' in temperature below the ~ 20 K inflection point, the theory[30] predicts that 0.5 T is actually not a low enough field to permit the observation of the relevant linearity effect, which is the key signature of the presence of d-wave superconductivity.[29] One must, therefore, conclude that the ''linearity'' seen at 0.5 T is *not* evidence of d-wave pairing, and that an alternative explanation (viz., flux pinning) of those data (especially the 0.5 T data) is required.

Moreover, the fortuitous low-temperature agreement shown in Fig. 2 of Ref. 26 between zero-field microwave data (taken from Ref. 23) and Sonier's 0.5 T μ^+SR data has often been erroneously cited as corroborating evidence for d-wave superconductivity. Since ''linearity'' with tempera-ture below 20 K and the purported agreement with the 0.5 T μ^+SR data do not, in fact, support the d-wave pairing,[30] the 0.5 T μ^+SR data actually negate the microwave data as evidence for d-wave pairing also.

B. Pairing and flux pinning

Clearly, the combination of the *nonmonotonic* behavior of $\lambda_{ab}(T \rightarrow 0, H)$ and the *inflection* in the data at ~ 20 K suggest that *at least two phenomena are affecting the data*. Rather than attempting to force the data to fit into the d-wave picture,[26–30] we take the approach that the deviations from s-wave behavior in Fig. 1 are due to quantifiable phenomena, most notably fluxon pinning and fluxon reordering, which were omitted by Sonier *et al.* Common sense would dictate that one first consider such flux-pinning effects in the context of ordinary s-wave pairing before proffering an intrinsic and unquantified d-wave-pairing (or higher angular-momentum pairing) picture. The clear sample dependency of the data exhibited in Fig. 1 implies the importance of *some* extrinsic effect.

The results presented in the next section correspond to the region in the vortex-state phase diagram where the fluxons form a solid-phase vortex lattice (see Fig. 4 of Ref. 48). Since the maximum temperature for the μSR data acquired at each field is 1 to 2 K below the vortex lattice melting temperature (the irreversibility boundary, namely the H vs T curve), the vortex lattice is subject to pinning. Therefore, we consider a model of temperature-activated flux pinning, as could occur in very clean crystals where the Abrikosov flux lattice becomes locked-in by weak pinning at oxygen vacancies and/or other defects.[49] As we shall show, the anomalous behavior shown in Fig. 1 is consistent with thermally activated vortex depinning which masks the true s-wave character of the underlying pairing state. We shall also argue that the underlying pairing symmetry cannot be d-wave, and in fact is s-wave.

C. Collective pinning model

As we analyze the data using a more sophisticated model than that in Fig. 1, it becomes desirable to treat instead of λ_{ab}, the total second moment due solely to vortex-lattice formation (without dipolar broadening) $\sigma(T, H)$, as defined by

$$\sigma = [\sigma_L^2 + \sigma_M^2]^{1/2}, \tag{6}$$

where the *smearing* parameter σ_M helps to model the additional broadening due to distortions of the vortex lattice, and σ_L is the square-root of the second moment of the *perfect* vortex-lattice distribution. The parameter σ_M is obtained by fitting the data with $G_{xx}(t)$ [Eq. (5)], and correcting for nuclear broadening by subtracting in quadrature the broadening, $\sigma_{dipolar}$, due to nuclear dipoles[50] (determined by fitting $\sigma_{dipolar}$ above T_c). For a triangular vortex-lattice geometry, σ_L is defined in terms of λ as[51,52]

$$\sigma_L^2 = [0.0609 \Phi_0 / \lambda^2]^2. \tag{7}$$

This is consistent with our choice of point vortices and a 0.1 nm cutoff. Here, $\Phi_0 = (hc/2e) = 2.068 \times 10^{-7}$ G cm^2 is the flux quantum.

The transformation to treating σ (rather than only λ) is necessary since, in the presence of perturbations (i.e., distortions due to flux pinning), the associated effects are reflected in *both* λ and σ_M. The notion that σ_M measures the distortion of the vortex lattice and λ is free of distortion effects is clearly untrue. This second moment $\sigma(T,H)$ incorporates (i) pinning and vortex motion, and (ii) an underlying pairing symmetry (either *s*-wave or *d*-wave). By applying our analysis in a self-consistent manner, we hope to determine the true nature of the underlying pairing state [i.e., $\lambda_{ab}(T,H)$], and to extract the London value of the penetration depth,

$$\lambda_{ab}(T=0,H=0) = [(m_{ab}^* c^2)/(4\pi n e^2)]^{1/2}, \quad (8)$$

where m_{ab}^* is the mean hole mass in the *a-b* plane, *c* is the speed of light, and *n* is the density of hole carriers. The penetration depth λ in Eq. (7) reduces to $\lambda_{ab}(T,H=0)$ for the ideal (nontriangular or oblique) vortex lattice.

1. Point and line vortex displacements

As in Ref. 52, we consider two types of vortex displacements: (i) shifts of the vortex *points* from their smooth *lines*, u_p, and (ii) shifts of the smooth *lines* from their positions in the flux-line lattice u_ℓ. The *point* distortions, u_p, tend to narrow the field distribution (i.e., decrease σ^2), while *line* distortions, u_ℓ, tend to broaden the distribution (i.e., increase σ^2). For arbitrarily large (uncorrelated) average displacements, $u = [u_p^2 + u_\ell^2]^{1/2}$, one obtains[52]

$$\sigma^2 \approx \sigma_0^2 [\exp(-26.3 u^2/a^2) + 24.8 \ln(\tilde{\kappa} u_\ell^2/a^2)]. \quad (9)$$

Here, the numerical factors come from Brandt's theory,[52] σ_0^2 is the second moment or variance of the field distribution for an ideal flux lattice, $\tilde{\kappa}^2 = (u_\ell^2 + 2\lambda_{ab}^2)/(u^2 + 4\xi_{ab}^2)$, $\xi_{ab} = \lambda_{ab}/\kappa$, κ is the Ginzburg-Landau parameter, and $a = (2\Phi_0/3^{1/2}B)^{1/2}$ is the vortex lattice parameter (*B* is the average local field).

At low applied magnetic fields, where the amplitude of the line distortion of a flux line, u_ℓ is small compared with the vortex lattice parameter *a*, one expects a minimal effect from such distortions. Likewise at high fields, where the intervortex interactions act to suppress the amplitude u_ℓ, one also expects a minimal effect. In contrast, point (or "fuzzy-core") distortions u_p are most dominant at low applied fields, where flux motion and vortex diffusion can occur, and at high fields, where small deviations of the individual fluxons from the flux line can be a significant fraction of the lattice parameter. Thus we expect a peak in line distortions u_ℓ and a minimum in point distortions u_p as a function of applied magnetic field *H*.

To show that the anomalous temperature and field dependences of σ are likely due to pinning effects, it is necessary to develop a self-consistent fit to the data for all four applied fields (simultaneously). To this end, we have adopted a fitting algorithm which incorporates a temperature- and field-dependent point disorder, u_p, and a field-dependent and

thermally-activated line disorder, u_ℓ. We further assume pinning by random, local pinning forces that induce deformations in the ideal vortex lattice. It has already been shown[51] that the increases in the second moment of the local field distribution, arising from sinusoidal fluctuations in the vortex density, scale with the pinning energy. Incorporating a wave vector dependence, which is modeled here by a distribution of pinning energies, we assume a pinning energy, *E*, that scales with the *line* fluctuations[51] as

$$E = \eta u_\ell^2, \quad (10)$$

where η is a proportionality constant. Allowing for a thermally activated temperature dependence,[53] the *line* pinning distortion u_ℓ is modeled in terms of its energy *E* according to the activation equation

$$u_\ell^2 = u_{\ell 0}^2 [1 - \exp(-E(u_\ell)/k_B T)], \quad (11)$$

where $u_{\ell 0}$ is the zero-temperature limit of u_ℓ. Equation (11) expresses the thermal transition from a uniform lattice in the limit of high temperature to a vortex lattice distorted by pinning at low temperature. The temperature dependence of u_ℓ is then found by solving the transcendental Eq. (11) above. The randomness and wave vector dependence of the relationship between *E* and u_ℓ are further incorporated into the model by convolving u_ℓ^2 with a Gaussian having a second moment of $u_{\ell 0}^2$ to better approximate pinning-well characteristics.

Point fluctuations along the flux lines are modeled by the parameter u_p. Brandt[52] treated the case of random point fluctuations of point vortices. In general, line waves along the flux lines increase the line tension and cost energy. The energy is supplied by pinning forces and by thermal energy which scales as $k_B T$. These two contributions are modeled for each field by two parameters, u_{p1} and u_{p2}, following the equation

$$u_p^2 = u_{p1}^2(H) + u_{p2}^2(H)(T/T_c). \quad (12)$$

D. *s*-wave picture with flux pinning

The theoretical form for fitting the $\sigma(T,H)$ data, as obtained from Eq. (6), was examined for various *s*-wave pairing models (*d*-wave pairing is discussed in the next section). The temperature dependence of $\lambda_{ab}(T,H=0)$ was tested for three values of the BCS theory coupling strength,[10,43] namely for the BCS coupling parameter $N(0)V = 0.4$, 1.0, and 4.0,[54] and for a two-fluid model expression.[34] [See Eq. (13).] The field dependence of $\sigma(T,H)$ was determined from the models based on Ginzburg-Landau theory presented in Refs. 42 and 52 and from models based on the quasiclassical Eilenberger theory[55] presented in Ref. 44. The penetration depth, $\lambda_{ab}(T,H=0)$, does not vary with *H* in these theories. But, the field dependence of the data critically enters into the fit to $\sigma(T,H)$. The best fit to the data (minimization of χ^2) is obtained with the field dependence of $\sigma(T,H)$ as calculated by Brandt,[52] which reduces to Eq. (1) for $H \ll H_{c2}$. A two-fluid model-like expression is used for the temperature dependence of the penetration depth:

TABLE I. Parameters of the fit of the two-fluid s-wave-based pinning model. Here we have $\langle u_p^2 \rangle = {}_0\int^{T_c} u_p^2(T)\, dT/T_c$.

Field (T)	Field-dependent parameters	
	$u_{\ell 0}/a$	$\langle u_p^2 \rangle^{1/2}/a$
0.05	0.031 (+0.061/−0.031)	0.204 (±0.012)
1.0	0.107 (+0.050/−0.067)	0.128 (±0.022)
3.0	0.088 (+0.034/−0.051)	0.087 (±0.030)
6.0	0.010 (+0.008/−0.010)	0.119 (±0.032)
Global parameters		
T_c	90.8 (±0.5) K	
$\lambda_{ab}(T=0, H=0)$	127.6 (±1.5) nm	
κ	43.8 (±1.8)	
Pinning "temperature" E/k_B	19.60 (+18.2/−12.2) K	
Reduced χ^2	2.38 (Chi-square per degree of freedom)	

$$\lambda_{ab}(T,H=0) = \lambda_{ab}(T=0,H=0)\ [1-(T/T_c)^\alpha]^{-1/2}, \quad (13)$$

which reduces to the two-fluid model for $\alpha = 4$.

Treating the exponent α as an adjustable parameter produces a χ^2 minimization with $\alpha = 4.16 \pm 0.20$. The best fit is statistically indistinguishable from the conventional two-fluid model, for which $\alpha = 4$. Thus Eq. (13) with $\alpha = 4.0$ is selected to model the temperature dependence of $\lambda_{ab}(T,H=0)$.

This work also examined several forms for the temperature dependence of the coherence distance, $\xi_{ab}(T,H=0)$. The fits presented below are obtained by fitting the data with a temperature-independent Ginzburg-Landau parameter, $\kappa = \lambda_{ab}(T,H=0)/\xi_{ab}(T,H=0)$. We found that fits using the $H_{c2}(T)$ functions given in Ref. 56, with $H_{c2}(0)$ taken to be a fitting parameter, produce comparably good χ^2 minimization, albeit with κ varying with temperature (κ increasing near T_c).

Table I shows the results for $\lambda_{ab}(T=0,H=0)$ and all the other parameters of our fit with s-wave pairing and fluxon pinning, as described above.

The curves shown in Fig. 2 represent the best fit to the $\sigma(T,H)$ data of our self-consistent pinning model. The fit is *global*, meaning that all four curves for the various fields were fit at the same time with one set of parameters in common. This yields a χ^2 per degree of freedom of 2.38 (based on statistical errors only), with the fitting parameters shown in Table I. Interestingly, the $\alpha = 4.0$ parameter in Eq. (13) shows that the best fit is consistent with strong coupling.

We have found with trial functions from extended BCS theory that the fit improves with increasing BCS coupling strength, $N(0)V$.[54] However, the simple form of Eq. (13), with α consistent with the two-fluid form, provides the best fit to the data. This is a very important result since, as the reader may recall, the two-fluid model[34] also best described the powders and early crystals.[4−7] Therefore the present data confirm our earlier assertion that the measurements before 1991 of the strongly pinned samples reflected the true underlying pairing state (i.e., strong-coupled s-wave pairing).

Figures 3(a) and 3(b) show the field-dependences of the line distortion parameter, $u_{\ell 0}$, and the temperature-averaged (rms) point distortion parameter, $\langle u_p^2 \rangle^{1/2} = [u_{p1}^2 + \frac{1}{2} u_{p2}^2]^{1/2}$, respectively, both normalized to the vortex-lattice spacing a. As predicted, point distortions are most important at low and high fields, whereas line distortions are important at intermediate fields. The contribution to the data arising from pinning effects can be removed using the fitted parameters. This elimination of the pinning effects also reveals results for the penetration depth. We define an *effective* penetration depth in the vortex state, e.g., as in Ref. 30, by the expression

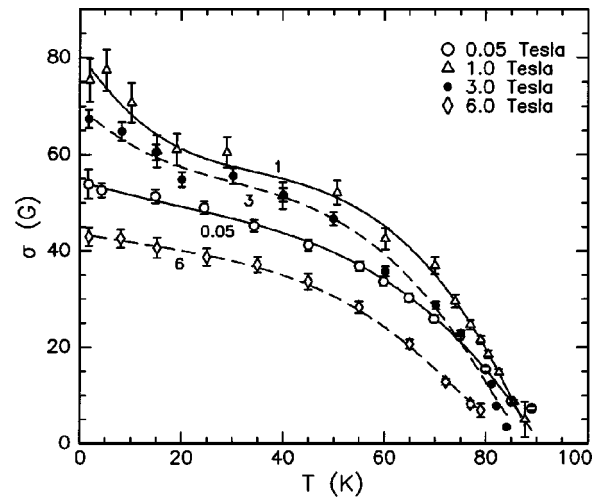$$\lambda_{ab}(T,H) = \lambda_{ab}(T,H=0)\ [\sigma(T,H)/\sigma(T,H=0)]^{-1/2}, \quad (14)$$

FIG. 2. The square-root of the second moment, σ, versus temperature, T, for single-crystal $YBa_2Cu_3O_7$ in applied fields of 0.05, 1.0, 3.0, and 6.0 T. The errors shown are statistical, corresponding to one standard deviation. The solid curves through the data represent the best (global) fit of our self-consistent pinning model with the underlying pairing function of Eq. (13), and $\alpha = 4$. The fitted parameters are given in Table I.
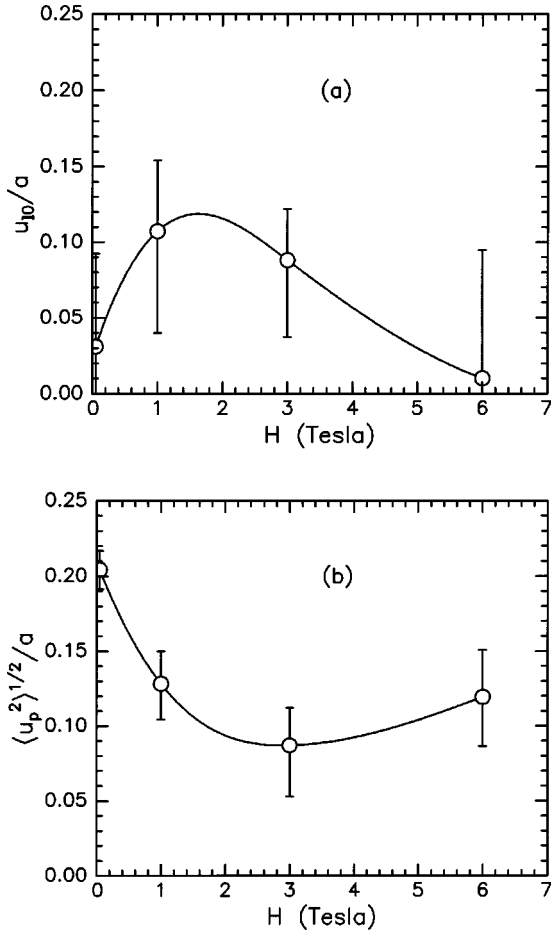
FIG. 3. The dependence on magnetic field of (a) the zero-temperature limit of the line distortion parameter, $u_{\ell 0}$, and (b) the root-mean-square average over $T \leqslant T_c$ of the point distortion, $\langle u_p^2 \rangle^{1/2}$, normalized to the vortex-lattice spacing a.

where $\lambda_{ab}(T,H=0)$ is the zero-field penetration depth, as given by the two-fluid model, and the ratio $\sigma(T,H)/\sigma(T,H=0)$ is the field dependence given by Ginzburg-Landau theory as calculated in Ref. 52. Experimental values of $\lambda_{ab}(T,H)$ and $\lambda_{ab}(T,H=0)$ are determined by comparing the individual data points for $\sigma(T,H)$ with the fitted theoretical function for $\sigma(T,H)$. The result for the zero-temperature, zero-field, London penetration depth is $\lambda_{ab}(T=0,H=0) = 127.6 \pm 1.5$ nm.

The result for the effective penetration depth, $\lambda_{ab}(T,H)$, is shown in Fig. 4(a). It is a monotonically increasing function of temperature and magnetic field. The result for $\lambda_{ab}(T,H=0)$, which is obtained as an extrapolation of each data point to zero applied field, is shown in Fig. 4(b). Clearly, the self-consistent agreement between the pinning theory detailed here, assuming an *s*-wave ground state, far exceeds the comparatively poor agreement found using the nonlocal *d*-wave theory of Ref. 30 (see Fig. 1).

E. *d*-wave picture with flux pinning

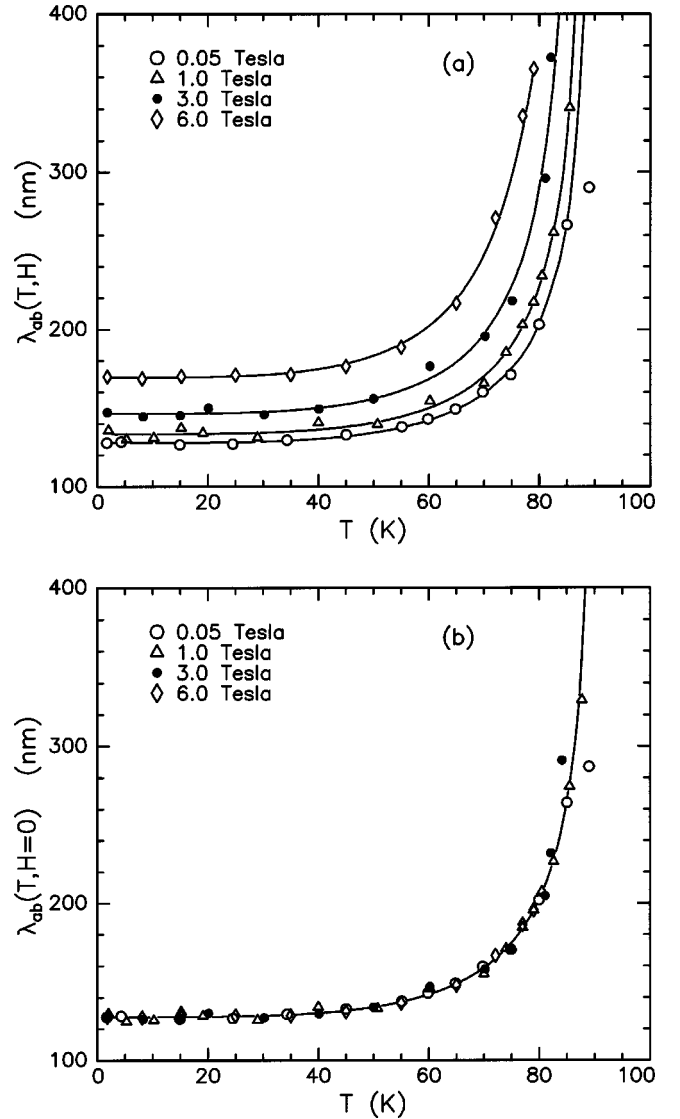We also attempted to incorporate the nonlocal *d*-wave pairing model of Ref. 30 into our pinning model. The

FIG. 4. The (a) temperature dependence of the *effective* magnetic penetration depth in the vortex state, $\lambda_{ab}(T,H)$, with the fitted effects of pinning removed. The curves through the data represent the *s*-wave pairing model of Eq. (13) with $\alpha = 4.0$ and magnetic field dependence model of Ref. 52. Frame (b) shows the temperature dependence of the zero-field penetration depth, $\lambda_{ab}(T,H=0)$, with the fitted effects of pinning removed. The curves are fitted with a London penetration depth of $\lambda_{ab}(T=0,H=0) = 127.6 \pm 1.5$ nm.

critical-field curve $H_{c2}(T)$ for *d*-wave pairing in Fig. 1 of Ref. 56 was used. In addition, we investigated the following modifications to improve the fits with the *d*-wave model function for $\sigma(T,H)$: (a) allowing an empirical effective shift in $T_c(H)$, which was not explicitly included in Ref. 30; (b) allowing $H_{c2}(0)$ to be a fitting parameter; and (c) taking κ to be a temperature-independent fitting parameter as in the *s*-wave model fits.

The *d*-wave model, with or without the modifications, generally yields extremely poor fits, having χ^2 per degree of freedom in the range 13 to 14 (as opposed to 2.38 for the *s*-wave model), which is significantly greater (worse) than that found for the two-fluid and BCS analyses above. The
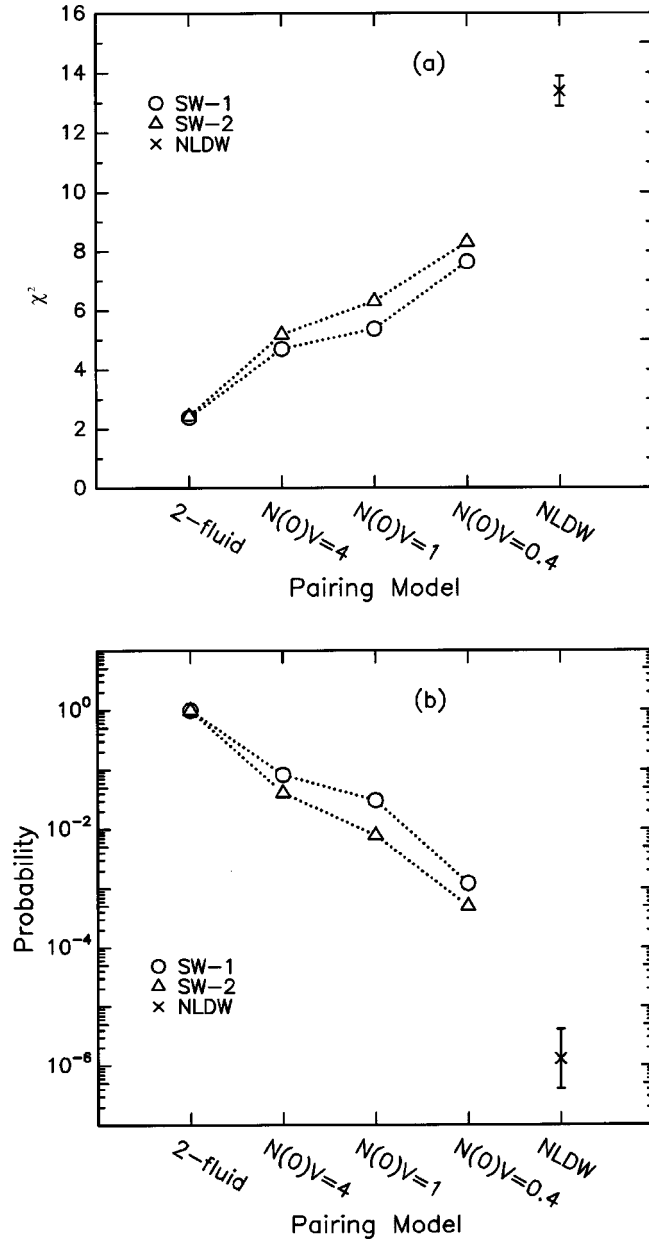
FIG. 5. (a) Results for chi-square (reduced χ^2) values, and (b) probability of statistical significance of the fits relative to the two-fluid s-wave pairing model, obtained from fitting $\sigma(T,H)$ with the vortex-lattice pinning model and various forms of superconducting pairing. The two-fluid model with s-wave pairing and magnetic field dependence as in Ref. 52 (SW-1) and as in Ref. 44 (SW-2), and BCS theory for couplings $N(0)V=4.0$, 1.0, and 0.4 also with pairing and magnetic-field dependences SW-1 and SW-2 are shown. The nonlinear d-wave model of Ref. 30 fit is denoted NLDW.

d-wave model fit yields $\lambda_{ab}=120.5\pm1.8$ nm and $T_c=90.6\pm0.7$ K.

The results for χ^2 are shown in Fig. 5(a) for various s-wave models of temperature and field dependence and the d-wave model from Refs. 30 and 56. Lower χ^2 values are obtained for the field dependence model of Ref. 52 (fits denoted SW-1), when compared with that of Ref. 44 (fits denoted SW-2). The minimum χ^2 is obtained for the SW-1 fit with the two-fluid model.

We use the F-distribution statistical analysis test to compare the χ^2 results shown in Fig. 5(a) for the s- and d-wave fits.[57] This test parameter is defined as $F=\chi_2^2/\chi_1^2$, where χ_1^2 is the chi-square for the two-fluid model s-wave fit SW-1, and χ_2^2 is the chi-square for any of the other model fits. The probability, P, for statistically random occurrence of the larger χ_2^2 for fits with any of the other models, when compared with the two-fluid s-wave model, is given by the expression

$$P= \int_F^\infty df \Gamma((\nu_1+\nu_2)/2)\Gamma^{-1}(\nu_1/2)\Gamma^{-1}(\nu_2/2)$$

$$\times(\nu_1/\nu_2)^{\nu_1/2}f^{(\nu_1-1)/2}(1+f\nu_1/\nu_2)^{(\nu_1+\nu_2)/2}, \quad (15)$$

where ν_1 and ν_2 are the number of degrees of freedom corresponding to χ_1^2 and χ_2^2, respectively. For the s-wave model, we have $\nu=37$; for the d-wave models ν is 36 to 38. Figure 5(b) shows the probability calculated according to Eq. (15) for each of the model fits. This statistical analysis finds that the probability for any d-wave model to give a better fit than the two-fluid model (also assuming s-wave pairing) is less than 4×10^{-6}.

The failure of the d-wave model can also be illustrated by plotting the residuals (i.e., the difference between the fitted theory and the data) for $\lambda_{ab}(T,H=0)$ for the nonlocal d-wave based pinning model, and comparing them with the residuals obtained assuming the underlying two-fluid form above. This is shown in Fig. 6, where the horizontal line at $\Delta\lambda_{ab}(T,H=0)$ denotes perfect agreement between theory and data. As is obvious, the strong-coupled s-wave assumption shown in Fig. 6(a) fits the data far better than the fit obtained assuming the d-wave model of Ref. 30 shown in Fig. 6(b). This is mainly due to the inability of the underlying d-wave model to deal with the absence of a linear temperature dependence in the 0.05 T data. Since the strong field dependence of the d-wave model comes primarily from the nonlocal contribution,[30] we are confident in concluding that an underlying d-wave pairing state (or any pairing state requiring nodes in the gap function) is entirely inconsistent with these data.

F. More problems with a d-wave interpretation

Experiments utilizing microwave cavity resonance,[58] ac susceptibility,[59] or rf resonance[60] have been executed on $YBa_2Cu_3O_7$ to test theoretical predictions of d-wave pairing theory for the nonlinear Meissner effect.[61,62] The predicted effects turned out to be either absent or unobservably small.[60] Moreover, the predicted fourfold symmetry in the ab plane for a $d_{x^2-y^2}$ order parameter is also found to be absent.[63]

In addition, the linear temperature dependence in the *change* of effective penetration depths, $\Delta\lambda_a$ or $\Delta\lambda_b$, in the ab plane of $YBa_2Cu_3O_7$ crystals, may not be actual evidence that the absolute penetration depths themselves, either λ_a or λ_b, underwent the required changes. In fact, the observed
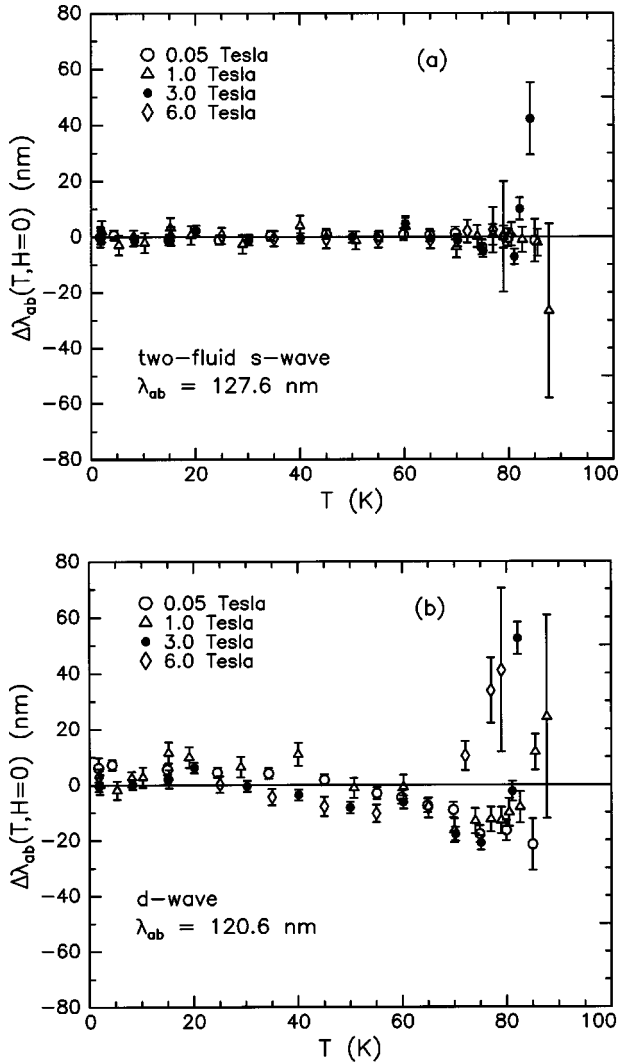
FIG. 6. Residual data $\Delta\lambda_{ab}(T,H=0)$ for $\lambda_{ab}(T,H\to 0)$, with the effects of pinning removed, assuming an underlying pairing state described by (a) the strong-coupled *s*-wave form of Eq. (13), and (b) the nonlocal *d*-wave model of Ref. 30.

changes may actually be due to defects, interrupted weak links, or other obstacles to supercurrent flow. Consequently, the results for $\Delta\lambda$ may have been generally overinterpreted in terms of Meissner screening currents purportedly flowing *unobstructed* along surfaces. Effects of current flow around the sample edges and along the *c* direction (*ac* or *bc* crystal faces) were generally assumed or argued not to be important, when there is some evidence that they are: In their LC (inductance-capacitance) resonance experiments with very weak rf probe fields, $<2\times10^{-7}$ T, Carrington *et al.* observed highly reproducible Fraunhofer-like oscillations in the field dependence of $\Delta\lambda_{ab}$, which they concluded are an indication of the presence of weak links on the edges of the crystal.[60] The field dependence of $\Delta\lambda$ observed by Carrington *et al.* and its temperature dependence were attributed by those authors to vortex motion. Moreover, in their analytical treatment of Meissner-London currents in superconductors, Brandt and Mikitik have cautioned that divergent surface currents at the samples' corners can nucleate quarter-

loop vortices and affect Meissner-effect measurements.[64,65] Thus, kinetic inductance of nascent vortex motion and transport through weak links are at least two extrinsic mechanisms that could cause a measurement of the effective penetration-depth difference $\Delta\lambda$ to be increased relative to the intrinsic $\Delta\lambda_a$ or $\Delta\lambda_b$. A key advantage of the μSR method is that the penetration depth is determined primarily by supercurrent flow on a microscopic scale in the bulk (around fluxons) and is insensitive to Meissner current flow over macroscopic sample dimensions.

IV. CONCLUSION

From the data and analyses presented here, along with the data of Sonier *et al.* and their comparison with the nonlocal *d*-wave theory of Ref. 30, it is clear that there is *no evidence* in any of the data for *d*-wave pairing. All of the modern data are, however, completely consistent with *temperature-activated vortex depinning, which masks an underlying s-wave (or extended s-wave) pairing state*. Strong-coupling theory and a two-fluid model describe the data well. Moreover, attempts to incorporate the nonlocal *d*-wave pairing function of Ref. 30 into the pinning model did not produce a satisfactory comparison with the data. Since the nonlocal aspect of this model[30] provides a stronger field dependence than that available from standard *d*-wave pairing schemes, it is safe to assume that *d*-wave pairing, even when coupled with pinning effects, cannot adequately explain the μSR data.

The effects of temperature-dependent, activated pinning of the type seen here were first observed (although much more pronounced) in *unannealed* $Bi_2Sr_2CaCu_2O_8$ single crystals.[11] In that case, a strong departure from *s*-wave behavior was observed at intermediate fields (0.3 and 0.4 T) due to flux motion and pinning, complete with an inflection in σ at about 15 K. As in the present case, the effects of temperature-dependent pinning were also suppressed in higher magnetic fields (in the $Bi_2Sr_2CaCu_2O_8$ case, 1.5 T), revealing the *s*-wave character of the underlying pairing function. Narrowing of the internal field distribution due to vortex disordering was also observed at 1.5 T. These same features are observed in the $YBa_2Cu_3O_7$ data presented here and elsewhere, and occur at higher fields due to the relatively stronger pinning energies present in $YBa_2Cu_3O_7$ crystals than found in *unannealed* $Bi_2Sr_2CaCu_2O_8$ crystals.

The presence of strong pinning of fluxons in the powder samples and early crystals actually allowed for a relatively accurate extraction of the ground state pairing symmetry (i.e., *s*-wave). In fact, the data almost always reflected two-fluid behavior, symptomatic of strong coupling. Unfortunately, as the quality of $YBa_2Cu_3O_7$ single-crystal samples improved to effectively match the quality of the available $Bi_2Sr_2CaCu_2O_8$ crystals, effects arising from temperature-dependent vortex motion and depinning became evident. While the occurrence of such phenomena in high-quality high-T_c materials was well reported[11] and widely cited,[28] the vortex-motion and depinning effects (which became more significant as the crystal-quality improved) were mistakenly attributed to *d*-wave superconductivity.[26–30] Since (i) few au-

thors realized that the superconductivity can be s-wave in the bulk and d-wave at the surface,[20] and (ii) surface-sensitive experiments providing evidence of *surface d*-wave superconductivity do *not* necessarily imply *bulk d*-wave superconductivity, some authors became confused about whether or not the bulk superconductivity was s-wave in character. The present work shows clearly that the pairing is s-wave in the bulk. In fact, all of the μSR data published to date which exhibit deviations from s-wave pairing, can readily be explained as resulting from temperature-activated depinning, which masks the true underlying s-wave character of the ground state symmetry.

A word about the microwave data: Sonier *et al.*[26] have shown in Fig. 2 of their paper that microwave measurements of $\lambda_{ab}(T,H)$ from Ref. 23 give very similar results to μSR data taken at low temperature in an applied field of 0.5 T. However, the microwave data cited match neither any other μSR data of Sonier *et al.*,[26] nor any data known. Indeed, there is no fundamental reason for the microwave data to compare well with *only* the 0.5 T μSR measurements of Ref. 26. Since the "linearity" of the low-temperature 0.5 T data cannot be due to d-waves, as discussed in Ref. 30, one can only conclude that the microwave work of Hardy *et al.*[23] does not necessarily represent sustainable evidence for d-wave pairing.

Thus, while our data do not rule out the possibility of *surface d*-wave effects, the evidence for our main point is overwhelming: the *bulk* superconductivity of $YBa_2Cu_3O_7$ (and, by inference, of $Bi_2Sr_2CaCu_2O_8$) is unquestionably s-wave in character, once temperature-activated depinning is taken into account.

Finally, we wish to comment about how this picture fits in with what many other authors believe: that the superconductivity is d-wave in character, with a prominent Cu d-wave signal, such as is evident in scanning tunneling microscopy (STM) data for $Bi_2Sr_2CaCu_2O_8$.[66] We doubt this d-wave interpretation of the superconductivity.[67,68]

Many probes, such as STM, detect d-wave behavior because they sense the *surface layers*, without determining if the detected layers are all superconducting. In contrast, muons detect only the *superconducting* carriers, and (because of the muon penetration depth) are especially sensitive to bulk layers more than to surface layers.

The surface of $Bi_2Sr_2CaCu_2O_8$ has a BiO layer, a SrO layer below it, and then a CuO_2 plane even below that. STM senses the BiO layer, the SrO layer beneath it, and that portion of the CuO_2 layer that consists of Cu d-states sticking up out of the cuprate plane into the SrO layer. STM senses a large d-wave component from the cuprate plane closest to the surface, which leads to the conclusion that if the cuprate planes superconduct, then the superconductivity is d-wave, not s-wave. This would be correct if the CuO_2 planes superconducted, and implies that the muons should also sense the CuO_2 planes, and hence should also exhibit d-wave behavior. But the μ^+SR data definitely do *not* exhibit d-wave behavior in $YBa_2Cu_3O_7$, and appear to behave similarly in $Bi_2Sr_2CaCu_2O_8$. This fact implies that the primary superconducting layers are *not* the cuprate planes.

Muons sense the superconducting carriers only, which are essentially pure s-wave in character experimentally, not d-wave. Their wave functions are nodeless. This means the superconducting layers are *not cuprate planes*, but are layers that have s-wave character, such as the SrO layers of $Bi_2Sr_2CaCu_2O_8$ or the BaO layers of $YBa_2Cu_3O_7$. If the superconductivity were in the CuO_2 planes, the muons (one would expect) would sense the d-waves of Cu, which they do not. Hence the fact that the muons sense essentially pure s-waves implies that the superconductivity is in other layers than the cuprate planes, such as the SrO or BaO layers.[68] We believe this reinterpretation to be consistent with the beautiful STM measurements of Davis's group, provided the primary superconductivity is assigned to the SrO layers, rather than to the cuprate planes.

*Permanent address.

[1] J. F. Annett, N. Goldenfeld, and S. R. Renn, in *Physical Properties of High Temperature Superconductors*, edited by D. M. Ginsberg (World Scientific, Singapore, 1991), Vol. 2, p. 571.

[2] J. F. Annett, N. Goldenfeld, and A. J. Leggett, in *Physical Properties of High Temperature Superconductors*, edited by D. M. Ginsberg (World Scientific, Singapore, 1996), Vol. 5, p. 375.

[3] J. F. Annett and J. P. Wallington, Physica C **341–348**, 1621 (2000).

[4] D. R. Harshman, G. Aeppli, E. J. Ansaldo, B. Batlogg, J. H. Brewer, J. F. Carolan, R. J. Cava, M. Celio, A. C. D. Chaklader, W. N. Hardy, S. R. Kreitzman, G. M. Luke, D. R. Noakes, and M. Senba, Phys. Rev. B **36**, 2386 (1987).

[5] B. Pümpin, H. Keller, W. Kündig, W. Odermatt, I. M. Savic, J. W. Schneider, H. Simmler, P. Zimmermann, J. G. Bednorz, Y. Maeno, K. A. Müller, C. Rossel, E. Kaldis, S. Rusiecki, W. Assmus, and J. Kowalewski, Physica C **162–164**, 151 (1989).

[6] B. Pümpin, H. Keller, W. Kündig, W. Odermatt, I. M. Savic, J. W. Schneider, H. Simmler, P. Zimmermann, E. Kaldis, S. Rusiecki, Y. Maeno, and C. Rossel, Phys. Rev. B **42**, 8019 (1990).

[7] D. R. Harshman, L. F. Schneemeyer, J. V. Waszczak, G. Aeppli, R. J. Cava, B. Batlogg, L. W. Rupp, Jr., E. J. Ansaldo, and D. Ll. Williams, Phys. Rev. B **39**, 851 (1989).

[8] A. G. Sun, D. A. Cajewski, M. B. Maple, and R. C. Dynes, Phys. Rev. Lett. **72**, 2267 (1994).

[9] R. A. Klemm, Int. J. Mod. Phys. B **12**, 2920 (1998), and references therein.

[10] J. Bardeen, L. N. Cooper, and J. R. Schrieffer, Phys. Rev. **106**,

162 (1957); **108**, 1175 (1957).

[11] D. R. Harshman, R. N. Kleiman, M. Inui, G. P. Espinosa, D. B. Mitzi, A. Kapitulnik, T. Pfiz, and D. Ll. Williams, Phys. Rev. Lett. **67**, 3152 (1991).

[12] D. A. Wollmann, D. J. Van Harlingen, J. Giapintzakis, and D. M. Ginsberg, Phys. Rev. Lett. **74**, 797 (1995).

[13] J. P. Rice, N. Rigakis, D. M. Ginsberg, and J. M. Mochel, Phys. Rev. B **46**, 11050 (1992).

[14] J. R. Kirtley, C. C. Tsuei, J. Z. Sun, C. C. Chi, Lock See Yu-Jahnes, A. Gupta, M. Rupp, and M. B. Ketchen, Nature (London) **373**, 225 (1995).

[15] J. R. Kirtley, C. C. Tsuei, K. A. Moler, J. Z. Sun, A. Gupta, Z. F. Ren, J. H. Wang, Z. Z. Li, H. Raffy, J. Mannhart, H. Hilgenkamp, B. Mayer, and Ch. Gerber, Czech. J. Phys. **46 (Suppl. S6)**, 3169 (1996).

[16] C. C. Tsuei, J. R. Kirtley, Z. F. Ren, J. H. Wang, H. Raffy, and Z. Z. Li, Nature (London) **387**, 481 (1997).

[17] C. C. Tsuei, J. R. Kirtley, M. Rupp, J. Z. Sun, A. Gupta, M. B. Ketchen, C. A. Wang, Z. F. Renn, J. H. Wang, and M. Bhushan, Science **271**, 329 (1996).

[18] C. C. Tsuei and J. R. Kirtley, Physica C **282−287**, 4 (1997).

[19] C. C. Tsuei, J. R. Kirtley, C. C. Chi, Lock See Yu-Jahnes, A. Gupta, T. Shaw, J. Z. Sun, and M. B. Ketchen, Phys. Rev. Lett. **73**, 593 (1994).

[20] K. A. Müller, J. Supercond. **15**, 319 (2002); Philos. Mag. Lett. **82**, 279 (2002).

[21] Qiang Li, Y. N. Tsay, M. Suenaga, R. A. Klemm, G. D. Gu, and N. Koshizuka, Phys. Rev. Lett. **83**, 4160 (1999).

[22] Q. Li, Y. N. Tsay, M. Suenaga, G. D. Gu, and N. Koshizuka, Physica C **282−287**, 1495 (1997).

[23] See, e.g., W. N. Hardy, D. A. Bonn, D. C. Morgan, R. Liang, and K. Zhang, Phys. Rev. Lett. **70**, 3999 (1993) and references therein.

[24] See, e.g., D. A. Bonn, R. Liang, T. M. Riseman, D. J. Barr, D. C. Morgan, K. Zhang, P. Dossanjh, T. L. Duty, A. McFarlane, G. D. Morris, J. H. Brewer, W. N. Hardy, C. Kallin, and A. J. Berlinsky, Phys. Rev. B **47**, 11314 (1993).

[25] J. D. Jorgensen, B. W. Veal, A. P. Paulikas, L. J. Nowicki, G. W. Crabtree, H. Claus, and W. K. Kwok, Phys. Rev. B **41**, 1863 (1990).

[26] J. E. Sonier, J. H. Brewer, R. F. Kiefl, G. D. Morris, R. I. Miller, D. A. Bonn, J. Chakhalian, R. H. Heffner, W. N. Hardy, and R. Liang, Phys. Rev. Lett. **83**, 4156 (1999).

[27] J. E. Sonier, J. H. Brewer, R. F. Kiefl, R. I. Miller, G. D. Morris, C. E. Stronach, J. S. Gardner, S. R. Dunsiger, D. A. Bonn, W. N. Hardy, R. Liang, and R. H. Heffner, Science **292**, 1691 (2001).

[28] J. E. Sonier, J. H. Brewer, and R. F. Kiefl, Rev. Mod. Phys. **72**, 769 (2000).

[29] Y. Wang and A. H. MacDonald, Solid State Commun. **109**, 289 (1998).

[30] M. H. S. Amin, M. Franz, and I. Affleck, Phys. Rev. Lett. **84**, 5864 (2000); **82**, 3232 (1999).

[31] See, e.g., T. J. Jackson, T. M. Riseman, E. M. Forgan, H. Glücklet, T. Prohscha, E. Morenzoni, M. Pleines, Ch. Niedermayer, G. Schatz, H. Luetkens, and J. Litterst, Phys. Rev. Lett. **84**, 4958 (2000).

[32] We shall normally refer to $YBa_2Cu_3O_{7-\delta}$ as $YBa_2Cu_3O_7$ when δ is small (less than 0.1), unless it is necessary to specify δ.

[33] This measurement also determined for the first time the anisotropy ratio of the effective mass along the c axis to the masses along the a and the b axes: $m_c^*/m_{ab}^* \geq 25$. See Ref. 7.

[34] W. Jones and N. H. March, *Theoretical Solid State Physics* (Wiley-Interscience, New York, 1973), Vol. 2, p. 895 *et seq.*

[35] See, e.g., J. Sonier, R. F. Kiefl, J. H. Brewer, D. A. Bonn, J. F. Carolan, K. H. Chow, P. Dosanjh, W. N. Hardy, R. Liang, W. A. MacFarlane, P. Mendels, G. D. Morris, T. M. Riseman, and J. W. Schneider, Phys. Rev. Lett. **72**, 744 (1994).

[36] For a review, see C. H. Pennington and C. P. Slichter, in *Physical Properties of High Temperature Superconductors II*, edited by D. M. Ginsberg (World Scientific, Singapore, 1990), p. 269.

[37] L. C. Hebel and C. P. Slichter, Phys. Rev. **107**, 901 (1957); **113**, 1504 (1959).

[38] L. Hebel, Phys. Rev. **116**, 79 (1959).

[39] A. Erb, "The impact of crystal growth, oxygenation and microstructure on the physics of rare earth (123) superconductors," thesis habilitation, University of Geneva, 1999.

[40] E. A. Lynton, *Superconductivity* (Methuen, London, 1962), Chap. III.

[41] See, e.g., A. Schenck, *Muon Spin Rotation Spectroscopy* (Hilger, Bristol, England, 1985).

[42] A. Yaouanc, P. Dalmas de Re'otier, and E. H. Brandt, Phys. Rev. B **55**, 11107 (1997).

[43] M. Tinkham, *Introduction to Superconductivity*, 2nd ed., (McGraw-Hill, New York, 1996), Chaps. 3 and 5, especially Eqs. 5−35.

[44] M. Ichioka, A. Hasegawa, and K. Machida, Phys. Rev. B **59**, 8902 (1999).

[45] The choice of a fixed core cutoff between 0.1 and 1.0 nm introduces negligible effect on the resulting fits.

[46] To facilitate the fitting, the following procedure was used for the 1.0, 3.0, and 6.0 T data: (i) the raw spectra from each of the four detectors (spaced ∼90° apart), $N_i(t)$ for $i = 1, 2, 3,$ and 4, were multiplied by $\exp(t/\tau_\mu)$; (ii) the average values of the resultant spectra, $\langle N_i(t)\exp(t/\tau_\mu)\rangle$, were obtained; (iii) the difference spectra, $A_i(t) = N_i(t)\exp(t/\tau_\mu) - \langle N_i(t)\exp(t/\tau_\mu)\rangle$ were then calculated; (iv) for convenience, especially at high fields, $A_i(t)$ were multiplied by $\cos(\omega_0 t)$ where ω_0 is the angular heterodyning frequency, to produce spectra with both rapid and slow oscillations; (v) the rapid oscillations were then eliminated by averaging over many time bins; and (vi) these "heterodyned" spectra were then fit with a similarly "heterodyned" fitting function.

[47] The established value of $\lambda_{ab}(0)$ is ≈120 to 140 nm.

[48] B. Billon, M. Charalambous, J. Chaussy, R. Kock, and R. Liang, Phys. Rev. B **55**, R14753 (1997).

[49] D. Nelson (private communication).

[50] The nuclear dipole contribution was determined by fitting the spectra above T_c assuming a Gaussian field distribution.

[51] E. H. Brandt, Phys. Rev. B **37**, 2349 (1988).

[52] E. H. Brandt, Phys. Rev. Lett. **66**, 3213 (1991).

[53] Thermally-activated flux creep was first considered by P. W. Anderson and Y. B. Kim, Rev. Mod. Phys. **36**, 39 (1964); P. W. Anderson, Phys. Rev. Lett. **9**, 309 (1962).

[54] $N(0)$ is the density of states at the Fermi energy and V is the pairing interaction in BCS theory (Ref. 10).

[55] G. Eilenberger, Z. Phys. **214**, 195 (1968).

[56] W. Kim, J.-X. Zhu, and C. S. Ting, Phys. Rev. B **58**, R607 (1998).

[57] P. R. Bevington, *Data Reduction and Error Analysis for the Physical Sciences* (McGraw-Hill, New York, 1969), Chap. 10.

[58] K. Zhang, D. A. Bonn, S. Kamal, R. Liang, D. J. Baer, W. N. Hardy, D. Basov, and T. Timusk, Phys. Rev. Lett. **73**, 2484 (1994).

[59] C. P. Bidinosto, W. N. Hardy, D. A. Bonn, and R. Liang, Phys. Rev. Lett. **83**, 3277 (1999).

[60] A. Carrington, R. W. Giannetta, J. T. Kim, and J. Giapintzakis, Phys. Rev. B **59**, R14173 (1999).

[61] S. K. Yip and J. A. Sauls, Phys. Rev. Lett. **69**, 2264 (1992).

[62] D. Xu, S. K. Yip, and J. A. Sauls, Phys. Rev. B **51**, 16233 (1995).

[63] A. Bhattacharya, I. Zutic, O. T. Valls, A. M. Goldman, U. Welp, and B. Veal, Phys. Rev. Lett. **82**, 3232 (1999).

[64] E. H. Brandt, Phys. Rev. Lett. **78**, 2208 (1997).

[65] E. H. Brandt and G. P. Mikitik, Phys. Rev. Lett. **85**, 4164 (2000).

[66] S. H. Pan, J. P. O'Neal, R. L. Badzey, C. Chamon, H. Ding, J. R. Engelbrecht, Z. Wang, H. Eisaki, S. Uchida, A. K. Gupta, K.-W. Ng, E. W. Hudson, K. M. Lang, and J. C. Davis, Nature (London) **413**, 282 (2001).

[67] J. D. Dow and D. R. Harshman, J. Low Temp. Phys. **131**, 483 (2003).

[68] J. D. Dow and D. R. Harshman, J. Phys. Chem. Solids **63**, 2309 (2002); Philos. Mag. B **82**, 1055 (2002).